

INVESTIGATION OF TWO PHOTON FINAL STATES IN e^+e^- ANNIHILATION AT $\langle\sqrt{s}\rangle = 34.2$ GeV

CELLO Collaboration

H.-J. BEHREND, Ch. CHEN¹, H. FENNER, U. GÜMPPEL, M.-J. SCHACHTER, V. SCHRÖDER, H. SINDT
Deutsches Elektronen-Synchrotron, DESY, Hamburg, Germany

G. D'AGOSTINI, W.-D. APEL, S. BANERJEE, J. BODENKAMP, J. ENGLER, G. FLÜGGE, D.C. FRIES,
W. FUES, K. GAMERDINGER, G. HOPP, H. KÜSTER, H. MÜLLER, H. RANDOLL,
G. SCHMIDT, H. SCHNEIDER
Kernforschungszentrum Karlsruhe and Universität Karlsruhe, Germany

W. De BOER, G. BUSCHHORN, G. GRINDHAMMER, P. GROSSE-WIESMANN, B. GUNDERSON,
C. KIESLING, R. KOTTHAUS, U. KRUSE², H. LIERL, D. LÜERS, H. OBERLACK, P. SCHACHT
Max-Planck-Institut für Physik und Astrophysik, München, Germany

P. COLAS, A. CORDIER, M. DAVIER, D. FOURNIER, J.F. GRIVAZ, J. HAISSINSKI, V. JOURNÉ,
A. KLARSFELD, F. LAPLANCHE, U. MALLIK, J.-J. VEILLET
Laboratoire de l'Accélérateur Linéaire, Orsay, France

J.H. FIELD³, R. GEORGE, M. GOLDBERG, B. GROSSETÊTE, O. HAMON, F. KAPUSTA, F. KOVACS,
G. LONDON, L. POGGIOLI, M. RIVOAL
Laboratoire de la Physique Nucléaire et Hautes Energies, Université de Paris, France

and

R. ALEKSAN, J. BOUCHEZ, G. CARNESECCHI, G. COZZIKA, Y. DUCROS, A. GAIDOT,
Y. LAVAGNE, J. PAMELA, J.P. PANSART and F. PIERRE
Centre d'Etudes Nucléaires, Saclay, France

Received 23 December 1982

Two photon final states in e^+e^- annihilation have been analyzed at CM energies around 34 GeV. Good agreement with QED is observed. Lower limits for the QED cutoff parameters of $\Lambda_+ > 59$ GeV and $\Lambda_- > 44$ GeV are determined. A search for two photons with missing energy yields an upper limit for the production of neutral particles which decay into a photon and a non-interacting particle. Constraints on the mass and the coupling strength of supersymmetric photinos are discussed.

The reaction $e^+e^- \rightarrow \gamma\gamma$ provides an important test of quantum electrodynamics (QED) in high energy e^+e^- reactions. It remains the only classical QED test

which — in contrast to lepton pair production — is not affected at lowest order by weak interactions and hadronic vacuum polarization [1]. Furthermore, in two photon final states one can search for pair production of neutral particles which decay into a photon and one non-interacting particle.

¹ Visitor from the Institute of High Energy Physics, Chinese Academy of Science, Peking, People's Republic of China.

² Visitor from the University of Illinois, Urbana, USA.

³ On leave of absence from DESY, Hamburg, Germany.

Experimental setup. The experiment was performed

using the CELLO detector at the e^+e^- storage ring PETRA. CELLO is a large solid angle detector with a solenoid spectrometer, electromagnetic calorimetry and muon identification. It has been described in detail elsewhere [2]; the liquid argon lead calorimeter which is essential for this analysis will be briefly presented.

The central part of the calorimeter consists of 16 modules and covers the polar angle range $|\cos \theta| < 0.86$. The end cap part comprises 4 modules and covers the polar angle range $0.98 > |\cos \theta| > 0.92$. The calorimeter has a depth of 20 radiation lengths with a fine lateral (~ 2 cm) and longitudinal (17 times) segmentation. The mean radial distance from the beam axis is 120 cm. An energy resolution of $13\%/\sqrt{E}$ and an angular resolution of ~ 6 mrad in azimuth and ~ 10 mrad in polar angle is achieved. One of the 16 central modules was not operating during the experiment.

Events used in this analysis were triggered by an energy deposition of greater than 2 GeV in each of two modules separated by at least 45° in azimuth. The resolution for the calorimeter trigger energy is $\sigma \sim 20\%$ for 2 GeV electrons. The trigger efficiency has been determined from Bhabha events and low energy electrons from higher order QED processes for which independent triggers from the track chambers and the calorimeter are available; after acceptance cuts the trigger efficiency is higher than 99%.

QED test. Compared to a previously published result [3] on the QED reaction

$$e^+e^- \rightarrow \gamma\gamma, \quad (1)$$

this analysis contains four times more events, the systematic error in the absolute normalization has been reduced to 3%, and a tin shield around the beam pipe which caused the conversion of at least one photon in $\sim 1/3$ of the events in the previous data was removed.

Events fulfilling the above trigger requirements were processed by reconstruction programs for charged particle tracks and electromagnetic showers.

The following selection criteria were applied:

- (1) Total shower energy more than 1.3 and less than 2.6 times beam energy E_b .
- (2) Number of reconstructed tracks less than two, or equal two with an opening angle of less than 10° (converted photons).

All events passing the cuts were scanned visually.

Bhabha events with hard photon radiation and an opening angle between the two tracks of less than 10° (0.9%) or with one track not reconstructed due to program and chamber inefficiencies (21.9%) as well as residual cosmic events (11.1%) were removed.

For the remaining events we used the information from the shower reconstruction and applied the following additional cuts:

- (3) At least two showers in the acceptance of the calorimeter modules.

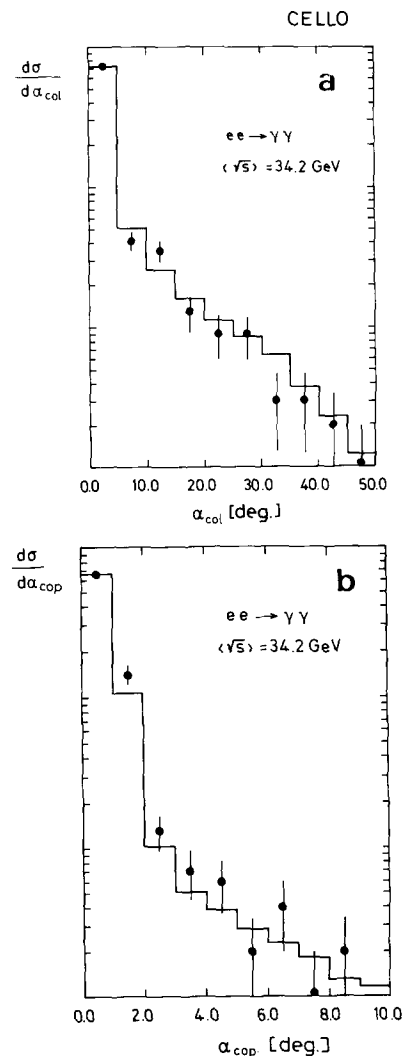


Fig. 1. The acollinearity (a) and acoplanarity (b) distributions for the reactions $ee \rightarrow \gamma\gamma(\gamma)$. The curves are the QED expectations up to order α^3 .

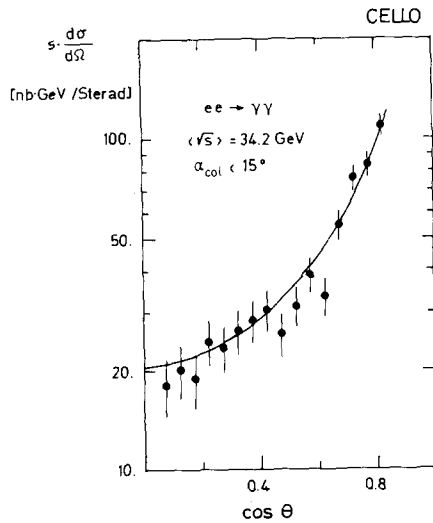


Fig. 2. The differential cross section $s d\sigma/d\Omega$ for the reaction $ee \rightarrow \gamma\gamma$ at $\langle\sqrt{s}\rangle = 34.2$ GeV. The curve is the QED expectation normalized to the Bhabha scattering process.

(4) Acollinearity between the two most energetic showers less than 15° .

Efficiencies of trigger, selection, and shower reconstruction were determined by a comparison with Bhabha scattering events. A correction for events with two converted photons was calculated from the amount of material in the beam pipe and the inner detector and was cross-checked with the number of events with one converted photon.

Radiative corrections were applied using a Monte Carlo generator [4] which includes corrections up to order α^3 . Figs. 1a and 1b show the acollinearity and acoplanarity distributions compared to the Monte Carlo prediction if cut (4) is removed.

The differential cross section with respect to the polar angle θ shown in fig. 2. The sample contains 1050 events for an integrated luminosity of 10.3 pb^{-1} . The data were normalized relative to Bhabha scattering in the polar angular range $0.75 < \cos \theta < 0.85$.

We obtain for the total cross section in the polar angle range $|\cos \theta| < 0.85$ for reaction (1) at $\sqrt{s} = 34.2$ GeV

$$\sigma_{\gamma\gamma} = 178.1 \pm 5.5 \text{ (stat.)} \pm 5.3 \text{ (syst.) pb,}$$

or in terms of the pointlike QED cross section

$$\sigma_{\text{exp}}/\sigma_{\text{QED}} = 0.962 \pm 0.031 \text{ (stat.)} \pm 0.030 \text{ (syst.).}$$

The systematic uncertainties are due to normalization (1.8%), radiative corrections (1%), and efficiency corrections (2.2%). They are added in quadrature.

For a quantitative comparison with possible QED violations, one usually introduces form factors into the differential cross section which are parametrized by the cutoff parameter Λ [5]. Assuming an additional heavy electron in the propagator, the differential cross section will take the form

$$\frac{d\sigma}{d\Omega} = \frac{\alpha^2}{s} \frac{1 + \cos^2\theta}{1 - \cos^2\theta} \left(1 \pm \frac{s^2}{2\Lambda_{\pm}^4} \sin^2\theta \right), \quad s = 4E_b^2.$$

To fit the data of fig. 2 with this expression we take Λ as free parameter and vary the normalization within the systematic error of the total cross section. We obtain the following lower limits for the cutoff parameter:

$$\Lambda_+ > 59 \text{ GeV}, \quad \Lambda_- > 44 \text{ GeV (95\% CL),}$$

$\Lambda_+ = M_{e^*}/g$ can be regarded as the ratio of the mass of a hypothetical heavy electron mediating the reaction and its coupling constant $g^{\pm 1}$.

Search for new neutral particles (photinos). The signature of two photons in the final state can also be used to search for unstable neutral particles which decay into a photon and another penetrating neutrino-like object. Such particles are, for instance, predicted as supersymmetric spin 1/2 partners [6] of the photon, called photinos (λ_γ). In e^+e^- annihilation, they can be pair produced in the reaction (cf. fig. 3):

$$e^+e^- \rightarrow \lambda_\gamma \bar{\lambda}_\gamma \rightarrow \gamma\gamma + \text{missing energy.} \quad (2)$$

Compared to the pair production of photons the cross section for reaction (2) may be substantially suppressed due to the mass of the exchanged object (a supersymmetric electron in the case of photinos). Therefore, even if the new particles are light, they may appear with detectable cross section only at high e^+e^- collision energies.

Depending on the mass of the photino m_{λ_γ} the signature for reaction (2) will change from two collinear photons with missing energy ($m_{\lambda_\gamma} \ll E_b$) to an acoplanar photon pair. Only part of the data at $\sqrt{s} = 34$ GeV with an integrated luminosity of 7.1 pb^{-1} has

^{#1} Similar results were obtained by other experiments [1].

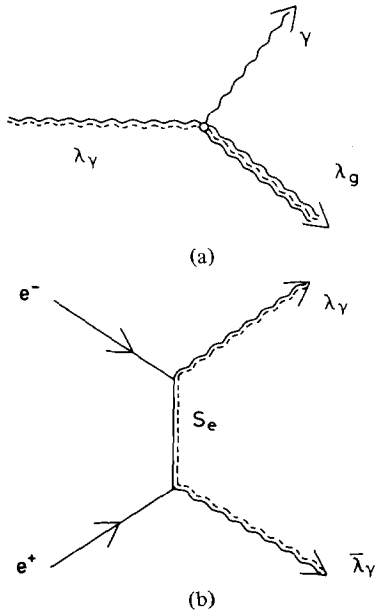


Fig. 3. (a) Decay of a massive photino into a photon and a supersymmetric gravitino (or goldstino). (b) Electron-positron annihilation into a photino-antiphotino pair. The exchanged particle is a scalar electron.

been used to search for these particles.

The following cuts were applied:

- (1) Two photons within the acceptance of the calorimeter modules and with $|\cos \theta_\gamma| < 0.825$.
- (2) No charged tracks.
- (3) Restriction on the shower energies ($x_\gamma = E_\gamma/E_b$):

$$x_{\gamma_1} x_{\gamma_2} < 0.5.$$

- (4) Acollinearity angle between the two showers less than 15° or:

- (4') Acoplanarity angle greater than 10° for acollinearity angle greater than 15° and the missing momentum vector pointing into the acceptance area of the calorimeter.

In addition, obvious cosmic ray events which were identified by the muon chambers and the direction of the two showers in the argon calorimeter were removed by a visual scan.

Cuts (3) and (4) suppress QED background from the reaction $ee \rightarrow \gamma\gamma(\gamma)$. Fig. 4 shows the correlation between the two photon energies E_{γ_1} and E_{γ_2} if cut (3) is not applied. No event candidate is observed.

The specific case of a supersymmetric photino is of

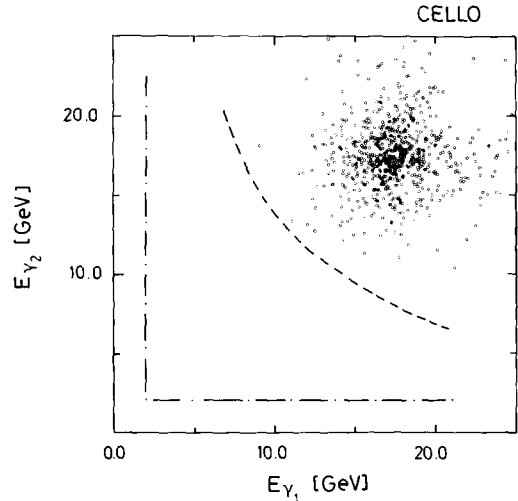


Fig. 4. Energy correlation for two collinear photons. The dotted line shows the energy cut applied in the search for unstable neutral particles which decay into a photon. The dotted-dashed line shows the trigger acceptance.

particular interest. If the photino is massive, it can decay into a gravitino (or goldstino) λ_g and a photon

$$\lambda_\gamma \rightarrow \lambda_g + \gamma,$$

with a lifetime [7]

$$\tau_{\lambda_\gamma} = 8\pi d^2 / m_{\lambda_\gamma}^5,$$

where m_{λ_γ} is the mass of the photino and d is a parameter characterizing the scale of the supersymmetry breaking.

In e^+e^- interactions, photino pairs are produced via the exchange of a scalar electron (fig. 3), and the differential cross section reads [8] (for $m_{\lambda_\gamma} \ll \sqrt{s}$)

$$\frac{d\sigma}{d\Omega} = \frac{\alpha^2 s}{16} \left(\frac{(1 - \cos \theta)^2}{[m_{s_e}^2 + \frac{1}{2}s(1 - \cos \theta)]^2} + \frac{(1 + \cos \theta)^2}{[m_{t_e}^2 + \frac{1}{2}s(1 + \cos \theta)]^2} \right).$$

m_{s_e} and m_{t_e} are the masses of the scalar electrons corresponding to the two helicity states of the electron.

In order to derive quantitative limits, even for heavy photinos, we have used the following approximation for the threshold behaviour of the differential cross section [9]

$$\frac{d\sigma}{d\Omega} = \frac{1}{16} \alpha^2 s (2\beta_{\lambda\gamma}^3 / m_{s_e}^4) (1 + \cos^2\theta),$$

where $\beta_{\lambda\gamma} = |p_{\lambda\gamma}|/E_b$. For simplicity we use $m_{s_e} = m_{t_e}$.

If the mass of the scalar electron is large compared to the CM energy, the production cross section rises $\sim s$. For a mass $m_{s_e} = 40$ GeV, the cross section for photino–antiphotino pair production rises from $R = \sigma_{\lambda\gamma\bar{\lambda}\gamma}/\sigma_{\mu\mu} \approx 10^{-3}$ at $s = 100$ GeV² to $R \approx 10^{-1}$ at $s = 1200$ GeV². To be compared to $R \approx 2.5$ for the reaction $ee \rightarrow \gamma\gamma$ in the polar angle range $|\cos\theta| < 0.825$.

From the non-observation of a collinear photon pair with missing energy we deduce a 95% CL upper limit of 1.1 pb for the cross section for the pair production of a light ($m_{\lambda\gamma} < 2$ GeV) photino–antiphotino pair decaying inside our detector ^{#2}.

The detectability depends on the mean pathlength, therefore we essentially measure $\tau_{\lambda\gamma}/m_{\lambda\gamma}$. In fig. 5a 95% CL upper limits for $\tau_{\lambda\gamma}/m_{\lambda\gamma}$ are shown for different photino masses versus the mass of the scalar electron. Assuming a mass $m_{s_e} = 40$ GeV, the lifetime of a photino with a mass of 100 MeV must be greater than 10^{-10} s. Fig. 5b shows the constraints on the mass of the photino and the scale parameter d which we can derive with the assumption $m_{s_e} = 40$ GeV. For fixed values of d , the observable number of events rises rapidly with the photino mass, because of the strong mass dependence of $\tau_{\lambda\gamma} \sim m_{\lambda\gamma}^{-5}$. For $d = (100 \text{ GeV})^2$ we exclude a photino in the mass range between ~ 100 MeV and ~ 13 GeV. The upper limit for the photino mass is dominated by the lifetime limit $\tau/m_{\lambda\gamma} \sim d^2/m_{\lambda\gamma}^6$, the lower limit by the kinematic limit for the production $\sigma_{\lambda\gamma\bar{\lambda}\gamma} \sim \beta_{\lambda\gamma}^3$. The lower limit is quite insensitive to a variation in the assumed scalar electron mass, as long as the rate limit is not achieved (with the present statistics we are sensitive to scalar electron masses less than 80 GeV). A change from $m_{s_e} = 40$ GeV to 20 or 60 GeV will change the lower mass limit by less than 20%.

Our experiment restricts the photino mass in a large range of the parameter d and the scalar electron mass m_{s_e} , especially in the region which is interesting for electroweak unification. From an experimental point

^{#2} A similar limit holds for massive unstable neutrino anti-neutrino pair production, if the neutrino decays into a photon and another neutrino.

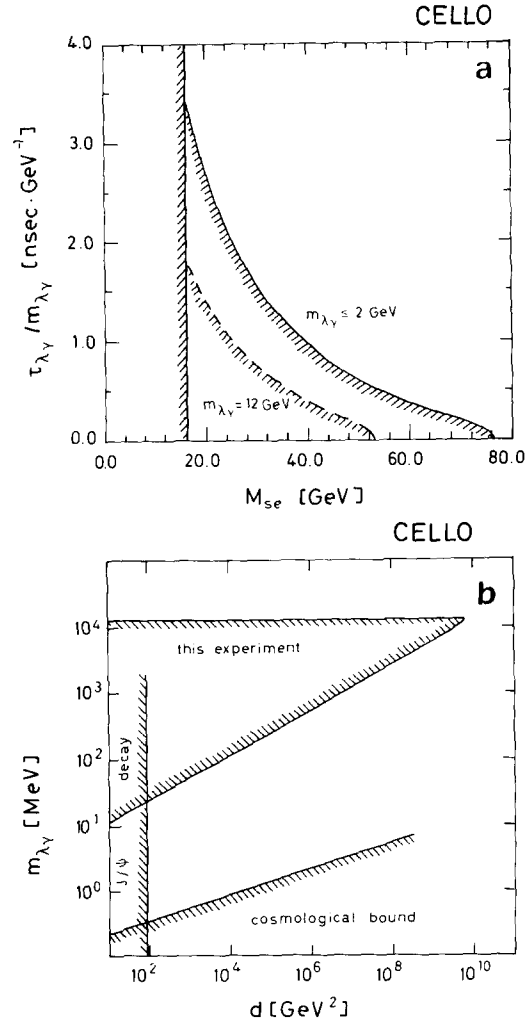


Fig. 5. (a) 95% CL lower limits on the lifetime to mass ratio of a heavy photino versus the mass of a scalar electron. The vertical line shows the limit for the scalar electron from ref. [10]. (b) 95% CL limits on the mass of a massive photino versus the scale parameter d ($m_{s_e} = 40$ GeV). The cosmological bound is discussed in refs. [7] and [11]. The limit from J/ψ decay is taken from ref. [12].

of view, we can conclude that scalar electron searches in the past probably were not affected by decaying photinos [10].

Summary. In summary, we have measured the reaction $ee \rightarrow \gamma\gamma$ at CM energies of ~ 34 GeV and have found good agreement with quantum electrodynamics. The total cross section in the angular range $|\cos\theta|$

< 0.85 is determined to be $\sigma_{\text{exp}} = \sigma_{\text{QED}}$ ($0.962 \pm 0.031 \pm 0.030$); lower limits for QED cutoff parameters $\Lambda^+ > 59$ GeV and $\Lambda^- > 44$ GeV are derived.

We have searched for neutral particles, which subsequently decay into a photon and a non-observable particle. A massive supersymmetric photino with masses of ~ 100 MeV to ~ 13 GeV is excluded over a large domain of scalar electron masses and symmetry breaking scale parameter d .

We are indebted to the PETRA machine group and the DESY computer center for their excellent support during the experiments. We acknowledge the invaluable effort of all the engineers and technicians of all the collaborating institutions in the construction and maintenance of the apparatus. The visiting groups wish to thank the DESY directorate for the support and kind hospitality extended to them. This work was partly supported by the Bundesministerium für Forschung und Technologie.

References

- [1] P. Dittmann and V. Hepp, DESY report 81/030; F.M. Renard, ECFA Study Week, DESY (Febr. 1977); JADE-Collab., W. Bartel et al., Phys. Lett. 92B (1980) 206; PLUTO-Collab., Ch. Berger et al., Phys. Lett. 94B (1980) 87; TASSO-Collab., R. Brandelik et al., Phys. Lett. 94B (1980) 259; MARK-J. Collab., D.P. Barber et al., Phys. Rev. Lett. 48 (1982) 967.
- [2] CELLO-Collab., H.-J. Behrend et al., Phys. Scr. 23 (1981) 610.
- [3] CELLO-Collab., H.-J. Behrend et al., Phys. Lett. 103B (1981) 148.
- [4] F.A. Berends and R. Kleiss, Nucl. Phys. B186 (1981) 22.
- [5] N.M. Kroll, Nuovo Cimento 45A (1966) 65; A. Litke, PhD thesis (1970) unpublished.
- [6] Kr.A. Gol'fan and E.P. Likhtman, JETP Lett. 13 (1971) 323; J. Wess and B. Zumino, Nucl. Phys. B70 (1974) 39; P. Fayet and S. Ferrara, Phys. Rep. 32C (1977) 249.
- [7] N. Cabibbo, G.R. Farrar and L. Maiani, Phys. Lett. 105B (1981) 155.
- [8] P. Fayet, LP TENS 82/12 (May 1982).
- [9] J. Ellis, private communication. β^3 factor is due to a p-wave transition.
- [10] CELLO-Collab., H.-J. Behrend et al., Phys. Lett. 114B (1982) 287.
- [11] J.E. Gunn et al., Astrophys. J. 223 (1978) 1015.
- [12] P. Fayet, Phys. Lett. 84B (1979) 421.